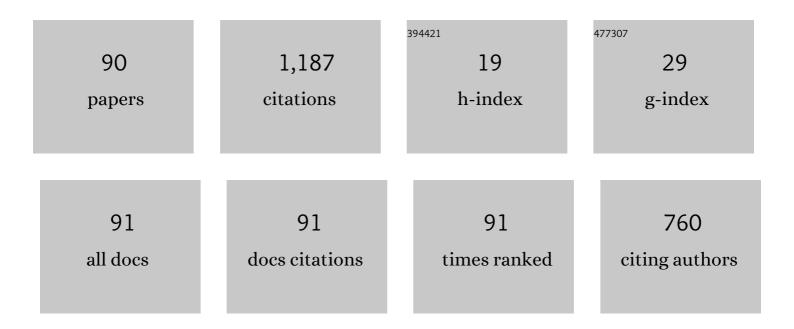
M F Ismail

List of Publications by Year in descending order

Source: https://exaly.com/author-pdf/847261/publications.pdf Version: 2024-02-01



MEISMAN

#	Article	IF	CITATIONS
1	Zinc oxide (ZnO) nanoparticles as saturable absorber in passively Q-switched fiber laser. Optics Communications, 2016, 381, 72-76.	2.1	85
2	A Stable Dual-wavelength Thulium-doped Fiber Laser at 1.9 μm Using Photonic Crystal Fiber. Scientific Reports, 2015, 5, 14537.	3.3	73
3	Using a black phosphorus saturable absorber to generate dual wavelengths in a Q-switched ytterbium-doped fiber laser. Laser Physics Letters, 2016, 13, 085102.	1.4	70
4	A Q-Switched Erbium-Doped Fiber Laser with a Carbon Nanotube Based Saturable Absorber. Chinese Physics Letters, 2012, 29, 114202.	3.3	67
5	S-band Q-switched fiber laser using MoSe 2 saturable absorber. Optics Communications, 2017, 382, 93-98.	2.1	51
6	Mode-locked thulium doped fiber laser with zinc oxide saturable absorber for 2â€Î¼m operation. Infrared Physics and Technology, 2019, 97, 142-148.	2.9	32
7	Tunable Q-switched thulium-doped Fiber Laser using multiwall carbon nanotube and Fabry-Perot Etalon filter. Optics Communications, 2017, 383, 359-365.	2.1	26
8	Ternary MoWSe <mml:math <br="" display="inline" xmlns:mml="http://www.w3.org/1998/Math/MathML">overflow="scroll" id="d1e463" altimg="si14.gif"><mml:msub><mml:mrow /><mml:mrow><mml:mn>2</mml:mn></mml:mrow></mml:mrow </mml:msub></mml:math> alloy saturable absorber for passively Q-switched Yb-, Er- and Tm-doped fiber laser. Optics Communications, 2019, 437, 355-362.	2.1	26
9	Q-switched ytterbium-doped fiber laser with zinc oxide based saturable absorber. Laser Physics, 2016, 26, 115107.	1.2	25
10	Tunable single wavelength erbium-doped fiber ring laser based on in-line Mach-Zehnder strain. Optik, 2016, 127, 8326-8332.	2.9	25
11	Q-switched fiber laser based on CdS quantum dots as a saturable absorber. Results in Physics, 2020, 16, 103123.	4.1	24
12	Evanescent field interaction of tapered fiber with graphene oxide in generation of wide-bandwidth mode-locked pulses. Optics and Laser Technology, 2017, 88, 166-171.	4.6	23
13	Mode-locked pulse generation in erbium-doped fiber laser by evanescent field interaction with reduced graphene oxide-titanium dioxide nanohybrid. Optics and Laser Technology, 2019, 118, 93-101.	4.6	22
14	Novel 3D-printed biaxial tilt sensor based on fiber Bragg grating sensing approach. Sensors and Actuators A: Physical, 2021, 330, 112864.	4.1	22
15	The performance of Ti2C MXene and Ti2AlC MAX Phase as saturable absorbers for passively mode-locked fiber laser. Optical Fiber Technology, 2021, 67, 102683.	2.7	22
16	155 nm-wideband and tunable q-switched fiber laser using an MXene Ti ₃ C ₂ T _X coated microfiber based saturable absorber. Laser Physics Letters, 2020, 17, 085103.	1.4	21
17	Q-switched Yb-doped fiber laser operating at 1073 nm using a carbon nanotubes saturable absorber. Microwave and Optical Technology Letters, 2014, 56, 1770-1773.	1.4	20
18	Tunable dual-wavelength thulium-doped fiber laser at 1.8Âμm region using spatial-mode beating. Journal of Modern Optics, 2015, 62, 892-896.	1.3	20

#	Article	lF	CITATIONS
19	Single and Double Brillouin Frequency Spacing Multi-Wavelength Brillouin Erbium Fiber Laser With Micro-Air Gap Cavity. IEEE Journal of Quantum Electronics, 2016, 52, 1-5.	1.9	19
20	Generation of mode-locked erbium-doped fiber laser using MoSe ₂ as saturable absorber. Optical Engineering, 2016, 55, 076115.	1.0	19
21	Titanium dioxide-based Q-switched dual wavelength in the 1 micron region. Chinese Optics Letters, 2016, 14, 091403-91407.	2.9	18
22	Molybdenum disulfide side-polished fiber saturable absorber Q-switched fiber laser. Optics Communications, 2017, 400, 55-60.	2.1	17
23	Aluminized Film as Saturable Absorber for Generating Passive Q-Switched Pulses in the Two-Micron Region. Journal of Lightwave Technology, 2017, 35, 2470-2475.	4.6	17
24	Graphene-PVA saturable absorber for generation of a wavelength-tunable passively Q-switched thulium-doped fiber laser in 2.0 <i>µ</i> m. Laser Physics, 2018, 28, 055105.	1.2	17
25	Multiwall carbon nanotube polyvinyl alcohol-based saturable absorber in passively Q-switched fiber laser. Applied Optics, 2014, 53, 7025.	1.8	16
26	Tunable 2.0 <i>µ</i> m Q-switched fiber laser using a silver nanoparticle based saturable absorber. Laser Physics, 2017, 27, 065110.	1.2	16
27	2µm mode-locked thulium-doped fiber laser using Mach–Zehnder interferometer tuning capability. Laser Physics, 2017, 27, 065104.	1.2	16
28	All-fiber multimode interferometer for the generation of a switchable multi-wavelength thulium-doped fiber laser. Applied Optics, 2017, 56, 5865.	1.8	16
29	Fabrication and Characterization of Microbent Inline Microfiber Interferometer for Compact Temperature and Current Sensing Applications. Journal of Lightwave Technology, 2017, 35, 2150-2155.	4.6	15
30	A combination of tapered fibre and polarization controller in generating highly stable and tunable dual-wavelength C-band laser. Journal of Modern Optics, 2017, 64, 709-715.	1.3	15
31	Molybdenum tungsten disulphide (MoWS ₂) as a saturable absorber for a passively Q-switched thulium/holmium-codoped fibre laser. Journal of Modern Optics, 2019, 66, 1163-1171.	1.3	14
32	Strain Sensor Based on Embedded Fiber Bragg Grating in Thermoplastic Polyurethane Using the 3D Printing Technology for Improved Sensitivity. Photonic Sensors, 2022, 12, 1.	5.0	13
33	Passively Q-switched thulium-doped fiber laser with silver-nanoparticle film as the saturable absorber for operation at 2.0 <i>ŵ</i> m. Laser Physics Letters, 2016, 13, 126201.	1.4	12
34	In ₂ Se ₃ saturable absorber for generating tunable Q-switched outputs from a bismuth–erbium doped fiber laser. Laser Physics Letters, 2018, 15, 115105.	1.4	12
35	Tunable passively Q-switched thulium-doped fiber laser operating at 1.9 μm using arrayed waveguide grating (AWG). Optics Communications, 2016, 380, 195-200.	2.1	11
36	Silicon-based microring resonators for multi-solitons generation for THz communication. Optical and Quantum Electronics, 2016, 48, 1.	3.3	10

#	Article	IF	CITATIONS
37	Investigation of structural and optoelectronic properties of n-MoS2/p-Si sandwiched heterojunction photodetector. Optik, 2019, 198, 163237.	2.9	10
38	Fabrication and characterization of tungsten disulphide/silicon heterojunction photodetector for near infrared illumination. Optik, 2019, 185, 819-826.	2.9	10
39	Tungsten-disulphide-based heterojunction photodetector. Applied Optics, 2019, 58, 4014.	1.8	10
40	A High-Precision Extensometer System for Ground Displacement Measurement Using Fiber Bragg Grating. IEEE Sensors Journal, 2022, 22, 8509-8521.	4.7	10
41	Passively Q-switched 1.3Âμm bismuth doped-fiber laser based on transition metal dichalcogenides saturable absorbers. Optical Fiber Technology, 2022, 69, 102851.	2.7	10
42	Seamless handover between WiMAX and UMTS. , 2009, , .		9
43	3D-Printed Tilt Sensor Based on an Embedded Two-Mode Fiber Interferometer. IEEE Sensors Journal, 2021, 21, 7565-7571.	4.7	9
44	Arc-shaped fiber coated with Ta2AlC MAX phase as mode-locker for pulse laser generation in thulium/holmium doped fiber laser. Optik, 2022, 252, 168508.	2.9	9
45	Application of MoS ₂ thin film in multi-wavelength and Q-switched EDFL. Journal of Modern Optics, 2017, 64, 457-461.	1.3	8
46	High sensitivity surface plasmon resonance (SPR) refractive index sensor in 1.5 μm. Materials Express, 2017, 7, 145-150.	0.5	8
47	Biaxial 3D-Printed Inclinometer Based on Fiber Bragg Grating Technology. IEEE Sensors Journal, 2021, 21, 18815-18822.	4.7	8
48	Mode-locked thulium/holmium-doped fiber laser with vanadium carbide deposited on tapered fiber. Optical Fiber Technology, 2021, 65, 102589.	2.7	8
49	Passively Q-switched S+/S band fiber laser with copper telluride saturable absorber. Laser Physics Letters, 2020, 17, 095102.	1.4	8
50	S-band Mode-locked Thulium-doped fluoride fiber laser using FePS3 as saturable absorber. Optical Fiber Technology, 2022, 72, 102985.	2.7	8
51	Visible Wireless Communications Using Solitonic Carriers Generated by Microring Resonators (MRRs). Iranian Journal of Science and Technology, Transaction A: Science, 2018, 42, 1595-1601.	1.5	7
52	70â€`nm, broadly tunable passively Q-switched thulium-doped fiber laser with few-layer Mo0.8W0.2S2 saturable absorber. Optical Fiber Technology, 2018, 46, 230-237.	2.7	7
53	Optically Modulated Tunable O-Band Praseodymium-Doped Fluoride Fiber Laser Utilizing Multi-Walled Carbon Nanotube Saturable Absorber [*] . Chinese Physics Letters, 2019, 36, 104202.	3.3	7
54	Compact L-band switchable dual wavelength SOA based on linear cavity fiber laser. Optik, 2019, 182, 37-41.	2.9	7

#	Article	IF	CITATIONS
55	Generation of four-wave mixing in molybdenum ditelluride (MoTe ₂)-deposited side-polished fibre. Journal of Modern Optics, 2021, 68, 425-432.	1.3	7
56	Tunable Spacing Dual-Wavelength Q-Switched Fiber Laser Based on Tunable FBG Device. Photonics, 2021, 8, 524.	2.0	7
57	All-incoherent wavelength conversion in highly nonlinear fiber using four-wave mixing. Optical Engineering, 2014, 53, 096112.	1.0	6
58	1.8 µm passively Q-switched thulium-doped fiber laser. Optics and Laser Technology, 2019, 120, 105757.	4.6	6
59	Soliton mode-locking in thulium-doped fibre laser by evanescent field interaction with reduced graphene oxide-titanium dioxide saturable absorber. Laser Physics Letters, 2019, 16, 075102.	1.4	6
60	Frequency switching multiwavelength Brillouin Raman fibre laser based on feedback power adjustment technique. Journal of Modern Optics, 2020, 67, 951-957. Al-tiberized, mode-locked laser at combinath xmlns:mml="http://www.w3.org/1998/Math/MathML"	1.3	6
61	display="inline" id="d1e95" altimg="si1.svg"> <mml:mrow><mml:mn>1</mml:mn><mml:mo>.</mml:mo><mml:mn>95</mml:mn><mml:msp: width="1em" class="nbsp" /><mml:mi mathvariant="normal">μ<</mml:mi><mml:mi mathvariant="normal">m</mml:mi </mml:msp: </mml:mrow> using copper chalcogenide Cu2Te-based	ace 2.1	6
62	evanescent field interaction. Optics Communications, 2020, 476, 126329. PERFORMANCE ANALYSIS OF COPPER TIN SULFIDE, Cu ₂ SnS ₃ (CTS) WITH VARIOUS BUFFER LAYERS BY USING SCAPS IN SOLAR CELLS. Surface Review and Letters, 2017, 24, 1750073.	1.1	5
63	Q-switched thulium/holmium fiber laser with gallium selenide. Optik, 2018, 175, 87-92.	2.9	5
64	Passive mode-locking in erbium-doped fibre laser based on BN-GO saturable absorber. Journal of Modern Optics, 2018, 65, 2339-2349.	1.3	5
65	Characterization of light-control-light system using graphene oxide coated optical waveguide. Laser Physics, 2018, 28, 076001.	1.2	5
66	Tunable single Stokes extraction from 20  GHz Brillouin fiber laser using ultranarrow bandwidth optical filter. Applied Optics, 2014, 53, 6944.	1.8	4
67	Dual-wavelength, passively Q-switched thulium-doped fiber laser with N-doped graphene saturable absorber. Optik, 2017, 149, 391-397.	2.9	4
68	Improvement of 2-μm Thulium-Doped Fiber Lasers via ASE Suppression Using All-Solid Low-Pass Photonic Bandgap Fibers. Journal of Lightwave Technology, 2019, 37, 5686-5691.	4.6	4
69	Configurable triple wavelength semiconductor optical amplifier fiber laser using multiple broadband mirrors. Microwave and Optical Technology Letters, 2020, 62, 46-52.	1.4	4
70	Ultrafast mode-locked dual-wavelength thulium-doped fiber laser using a Mach-Zehnder interferometric filter. Opto-electronics Review, 2018, 26, 312-316.	2.4	3
71	Mode-locked near-infrared thulium doped fibre laser using evanescent field effect with Bi ₂ O ₃ saturable absorber. Laser Physics, 2019, 29, 055104.	1.2	3
72	Q-switched Thulium-doped fiber laser at 1860â€ [−] nm and 1930â€ [−] nm using a Holmium-doped fiber as an amplified spontaneous emission filter. Optics and Laser Technology, 2020, 123, 105908.	4.6	3

#	Article	IF	CITATIONS
73	Tunable mode-locked soliton fibre laser based on single-walled carbon nanotubes. Quantum Electronics, 2018, 48, 930-935.	1.0	3
74	Graphene oxide (GO)-based wideband optical polarizer using a non-adiabatic microfiber. Journal of Modern Optics, 2017, 64, 439-444.	1.3	2
75	Generation of sub-nanosecond pulse in dual-wavelength praseodymium fluoride fibre laser. Laser Physics, 2019, 29, 105101.	1.2	2
76	Passively Q-switched thulium fluoride fiber laser operating in S-band region using N-doped graphene saturable absorber. Indian Journal of Physics, 2020, 95, 1837.	1.8	2
77	Investigation of ellipticity and pump power in a passively mode-locked fiber laser using the nonlinear polarization rotation technique. Chinese Optics Letters, 2017, 15, 051402-51406.	2.9	2
78	Temperature-independent vibration sensor based on Fabry–Perot interferometer using a fiber Bragg grating approach. Optical Engineering, 2022, 61, .	1.0	2
79	Supercontinuum generation from a sub-megahertz repetition rate femtosecond pulses based on nonlinear polarization rotation technique. Journal of Modern Optics, 2014, 61, 1333-1338.	1.3	1
80	Surface plasmonic effect of nanoparticle-like silver nanostructure on the high responsivity of visible/infrared silver-based heterojunction photodetector. Journal of Modern Optics, 2019, 66, 1329-1338.	1.3	1
81	Narrow bandwidth optimization using a polymer microring resonator in a thulium–holmium fiber laser cavity. Optics Communications, 2020, 466, 125574.	2.1	1
82	Tunable Q-switched ytterbium-doped fibre laser with Nickel Oxide saturable absorber. Indian Journal of Physics, 2021, 95, 361-366.	1.8	1
83	Isolator-free, widely tunable thulium/holmium fiber laser. Malaysian Journal of Fundamental and Applied Sciences, 0, 14, 439-442.	0.8	1
84	Implementing a reconfigurable MAP decoder on a soft core processor system. , 0, , .		0
85	Uplink call admission control with adaptive bit rate degradation for WCDMA. , 2009, , .		0
86	Four-wave mixing analyses for future ultrafast wavelength conversion at 0.64     Tb / s in a semiconductor optical amplifier. Optical Engineering, 2014, 53, 116111.	1.0	0
87	Analysis of semiconductor InGaAsP/InP coupled microring resonators (CMRR) by time-domain travelling wave (TDTW) method. Journal of Optics (India), 2017, 46, 311-319.	1.7	0
88	Bidirectional-pumped tunable fiber laser using a voltage-controlled Fabry-Perot Etalon filter. Malaysian Journal of Fundamental and Applied Sciences, 2017, 13, .	0.8	0
89	MoSSe-based passively modulated erbium doped fiber laser. Laser Physics, 2020, 30, 095104.	1.2	0
90	Enhancement of four-wave mixing and supercontinuum generations aided with dual arc-shaped fiber with 2D material. IEEE Journal of Quantum Electronics, 2022, , 1-1.	1.9	0